SCIENTIFIC REPORTS

OPEN

CONFERENCE PROCEEDINGS

ISFM2014

Engineering Bi_2O_3-Bi_2S_3 heterostructure for superior lithium storage

Tingting Liu*, Yang Zhao*, Lijun Gao & Jiangfeng Ni

College of Physics, Optoelectronics and Energy & Collaborative Innovation Center of Suzhou Nano Science and Technology, Soochow University, Suzhou 215006, China.

SUBJECT AREAS:

MATERIALS FOR ENERGY AND CATALYSIS

BATTERIES

Received
17 October 2014

Accepted
14 November 2014

Published
23 March 2015

Correspondence and requests for materials should be addressed to LG. (gaolijun@suda.edu.cn) or JN. (jeffni@suda.edu.cn)

* These authors contributed equally to this work.

Bismuth oxide may be a promising battery material due to the high gravimetric (690 mAh g^{-1}) and volumetric capacities (6280 mAh cm^{-3}). However, this intrinsic merit has been compromised by insufficient Li-storage performance due to poor conductivity and structural integrity. Herein, we engineer a heterostructure composed of bismuth oxide (Bi_2O_3) and bismuth sulphide (Bi_2S_3) through sulfurization of Bi_2O_3 nanosheets. Such a hierarchical Bi_2O_3-Bi_2S_3 nanostructure can be employed as efficient electrode material for Li storage, due to the high surface areas, rich porosity, and unique heterogeneous phase. The electrochemical results show that the heterostructure exhibits a high Coulombic efficiency (83.7%), stable capacity delivery (433 mAh g^{-1} after 100 cycles at 600 mA g^{-1}) and remarkable rate capability (295 mAh g^{-1} at 6 A g^{-1}), notably outperforming reported bismuth based materials. Such superb performance indicates that constructing heterostructure could be a promising strategy towards high-performance electrodes for rechargeable batteries.

In order to meet the requirement for high energy density, development of battery materials with large capacity has been urgently desired[1]. Alloying anode materials, such as Si, Sn, Sb, Bi and their compounds, can supply Li-storage capacity significantly beyond that of commercial graphite. Thus, they have been extensively explored as alternative materials for rechargeable Li batteries[2]. Among these materials, Bi-based materials have attracted considerable attention owing to their high pack density and volumetric capacity. For instance, Bi is able to afford a volumetric capacity of 3760 mAh cm^{-3}, which is 4.5-fold that of graphite anode[3,4]. Besides metallic Bi, bismuth compounds such as sulfide (Bi_2S_3) and oxide (Bi_2O_3) could be promising electrode materials towards Li storage. Specifically, considerable effort has been devoted to the development of advanced Bi_2S_3 electrodes in recent. By tuning the structure, surface, and compositing, researchers could develop high-performance Bi_2S_3 materials[5–7]. However, few works have been focused on the oxide counterpart Bi_2O_3, although the oxide possesses a higher theoretical capacity[8].

Similar to Bi_2S_3, bismuth oxides (Bi_2O_3) are layered semiconductor (band gap = 2.8 eV). This structure can be described as a succession of alternating layers of bismuth atoms parallel to the (100) plane of the cell, and oxide ions in the c-axis direction[9]. Resulting from direct band gap structure and remarkable photoluminescence properties, Bi_2O_3 could be promising for various applications, including gas sensors, solid oxide fuel cells, and photocatalyst for water splitting and pollutant decomposing[10–13]. Particularly, the intriguing layered structure enables it to be an interesting host for energy storage such as hydrogen and lithium.

Li-storage behaviour of Bi_2O_3 was firstly evaluated by Temperoni *et al.* more than 30 years ago. A high capacity of 660 mAh g^{-1} was achieved in the $LiAsF_6$-THF electrolyte, suggesting that the reaction involved both the conversion and alloying process (Eq. 1)[14].

$$Bi_2O_3 + 12Li \leftrightarrow 3Li_2O + 2Li_3Bi \quad (1)$$

Thus, the theoretical capacity for Bi_2O_3 reaches 690 mAh g^{-1} and 6280 mAh cm^{-3}, much greater than that of commercial graphite (372 mAh g^{-1} and 820 mAh cm^{-3}). However, the reversibility of Bi_2O_3 electrode is a major issue. Recently, Luo *et al.* revisited Bi_2O_3 anode by directly growing Bi_2O_3 nanoparticles on nickel foam[8]. The resulting Bi_2O_3/Ni exhibited impressive Li-storage reversibility, retaining 782 mAh g^{-1} over 40 cycles at 100 mA g^{-1}, and affording 668 mAh g^{-1} at a higher rate of 800 mA g^{-1}. Nevertheless, neither long-term cycling stability nor high-rate capability is sufficient for practical application. Adoption of heavy Ni foam substrate also causes substantial loss of the battery energy. It is imperative to further enhance rate and cycle capability of the material while maintaining higher energy density.

Battery materials usually have to be operated for hundreds and even thousands of cycles. To fulfil such a stringent requirement, the electrode materials need to be well engineered. Various strategies such as engineering hierarchical structures[15,16], surface wiring[17,18], and phase and composition modification[19,20] have been reported to efficiently tune the material property. Among the available strategies, constructing heterogeneous materials has received significant attention due to synergetic effect[21,22]. The heterostructure would take profit of the components and their interaction, thus outperforming any single component[23,24]. Particularly, heterostructures composed of both sulphide and oxide is very promising in energy related fields, due to improved performance and ease of fabrication[25–27]. Although heterogeneous bismuth materials have shown excellent optical property[13,28], their Li-storage have not been explored. In this work, we demonstrate that superior lithium storage could be realized by engineering a Bi_2O_3-Bi_2S_3 heterostructure (denoted as BO-BS). The BO-BS can be facilely fabricated through sulfurization of Bi_2O_3 with the assistance of thioacetamide (TAA). The hierarchical BO-BS heterostructure exhibits unique structural features such as high surface areas, rich porosity, and intrinsic flexibility, which can be utilized for excellent Li storage.

Results

Synthesis of the Bi_2O_3-Bi_2S_3 heterostructure is schematically illustrated in Figure S1. Firstly, the Bi_2O_3 phase was formed immediately when $Bi(NO_3)_3$ species were irradiated by sonication. The Bi_2O_3 phase exhibited sheet structure, due to the directing effect of CTAB surfactant. Then, the Bi_2O_3 phase would combine H_2S molecules, which were gradually released through hydrolysis of TAA, and then partial Bi_2O_3 species would be transformed into Bi_2S_3. By controlling the sulfurization time, a heterostructure consisting of Bi_2O_3 and Bi_2S_3 with certain ratio would be achieved.

Morphologies of the prepared Bi_2O_3 and BO-BS heterostructure revealed by scanning electron microscopy (SEM) and transmission electron microscopy (TEM) are illustrated in Figure 1. Figure 1a and b show that the Bi_2O_3 displays a microsphere structure composed of ultrathin nanosheets with thickness of several nanometers. Due to nature of laminar structure, the Bi_2O_3 tends to be sheet-shape, even for products without using surfactants (Figure S2). Nonetheless, the CTAB-directed nanosheets are thinner and smoother in nature. After sulfurization, the sphere-like structure is largely reserved, but the nanosheets become thicker and coarsened (Figure 1c, d). A TEM image reveals that the sheets actually consist of two parts, wrinkled sheets supported on smooth sheet substrates (Figure 1e). This structure was further characterized by high-resolution TEM imaging, as shown in Figure 1f. The smooth sheet substrate shows clear lattice fringes with interplanar distance of 0.32 nm, which corresponds to (111) facet of cubic Bi_2O_3. The corrugated sheets exhibit a lattice fringe of 0.79 nm, correlating with (110) facet of orthorhombic Bi_2S_3. Thus, the final sample is a heterostructure comprised of Bi_2O_3 and Bi_2S_3. The coarsening and corrugation of Bi_2S_3 sheets may results from the lattice mismatch between cubic and orthorhombic phases.

The phase of the heterostructure was identified by XRD, as shown in Figure 2a. The as-prepared sample shows poorly crystalline characteristic. Although diffraction peaks due to cubic Bi_2O_3 can be clearly confirmed (PDF #52-1007), peaks due to orthorhombic Bi_2S_3 phase are barely visible, suggesting the latter phase is still in an amorphous or nanocrystalline state. Generally, cubic Bi_2O_3 (δ-Bi_2O_3) is the high temperature stable form and often obtained at a temperature above 700°C. In this case, however, the cubic phase can be successfully obtained even at room temperature using ultrasonication. After annealing at 200°C for 1 hour, well crystallized Bi_2S_3 phase emerges (PDF #17-0320), agreeing with our previous work[5]. Composition and microstructure of the product were characterized by Energy dispersive X-ray spectroscopy (EDX) and Fourier transform infrared spectroscopy (FTIR). EDX shown in Figure 2b reveals that the heterostructure contains Bi, O, and S elements, and the molar ratio between O and S elements is ~1.1 : 1. Certainly, the ratio can be readily tuned by varying the synthesis time, e.g. 9 : 1 for 1 hour and 4 : 1 for 2 hours. In the FTIR spectra presented in Figure 2c, the bands at 461, 528, and 619 cm^{-1} can be assigned to Bi–O or Bi–S. The band at 1382 cm^{-1} is assigned to C–OH stretching vibrations, while the bands in the range of 1124–1020 cm^{-1} may be due to C–O vibrations[7]. Existence of these bands suggests that some TAA and CTAB molecules are absorbed onto the BO-BS product. Figure 2d presents the N_2 adsorption isotherms of the BO-BS, revealing a high surface area of 21.2 $m^3\ g^{-1}$ and enriched mesoporous characteristic of 0.122 $cm^3\ g^{-1}$.

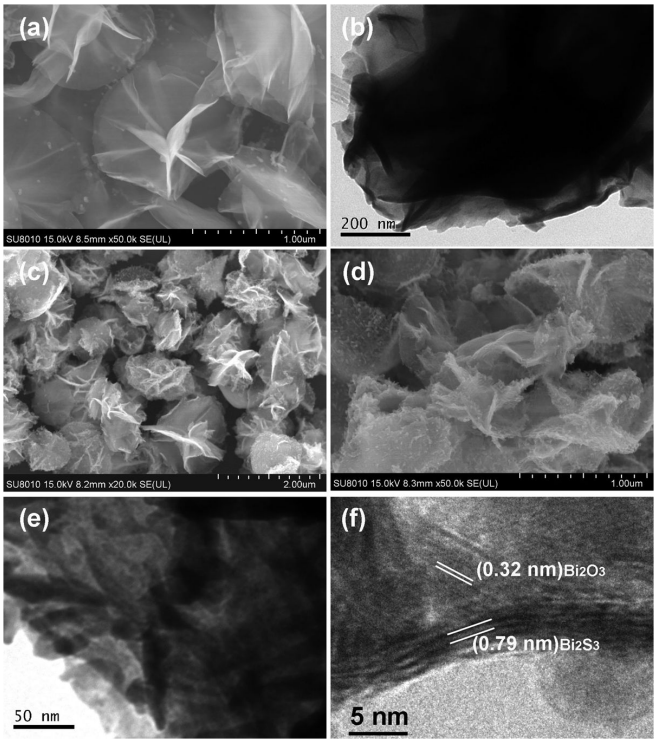

Figure 1 | SEM and TEM images of Bi_2O_3 and Bi_2O_3-Bi_2S_3 heterostructure. (a) SEM and (b) TEM images of Bi_2O_3. (c, d) SEM and (e, f) TEM images of Bi_2O_3-Bi_2S_3 heterostructure.

Such a porous heterostructure can be employed as an efficient electrode for Li storage. Figure 3a shows the galvanostatic charge and discharge curves of BO-BS during initial cycles. At a rate of 60 mA g^{-1}, the initial discharge and charge capacities of BO-BS are 1257 and 1052 mAh g^{-1}, respectively. The Coulombic efficiency of 83.7% surpasses those for bismuth based electrodes (60–70%, Figure S3)[5–8] and is even comparable to that for carbonaceous insertion anodes[29]. Such a high efficiency may be closely related to strong interaction between bismuth oxide and sulfide in the heterostructure. As shown in Figure 3a, the initial discharge plateau at ~1.7 V reflecting conversion process is almost lost. As the conversion reaction is usually poorly reversible, thus elimination of this plateau would lead to enhanced reversibility and Coulombic efficiency. Note that the high efficiency is critical for the current battery configuration, because Li source is usually supplied by low-capacity cathodes. The Coulombic efficiency further increases to 95% during the following cycles, while the capacity stabilizes at ~1072 mAh g^{-1}. Such a capacity exceeds the theoretical value of the BO-BS heterostructure (658 mAh g^{-1})[8], which could be explained by taking the large surface area and rich porosity into consideration[28].

Li-storage property of the heterostructure was electrochemically probed by cyclic voltammetry (CV), and the results are presented in

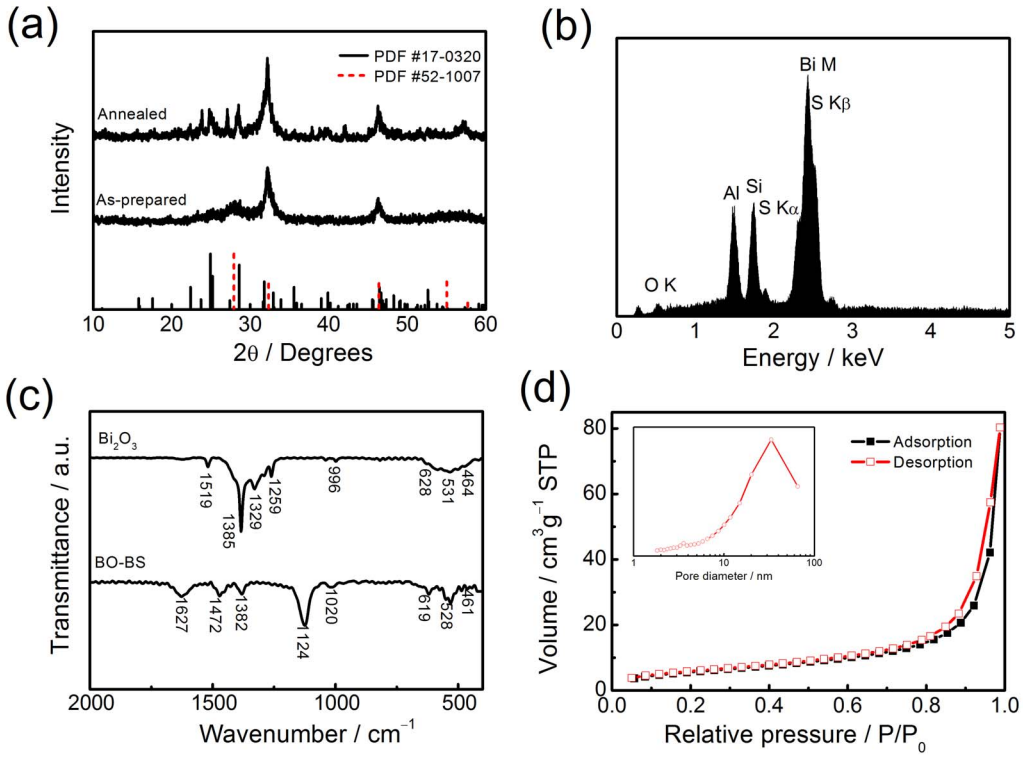

Figure 2 | (a) XRD patterns and (b) EDX of BO-BS heterostructure. Al and Si signals are due to the sample holder. (c) FTIR of BO-BS and Bi_2O_3. (d) N_2 adsorption and desorption isotherms and pore size distribution (inset) of BO-BS heterostructure.

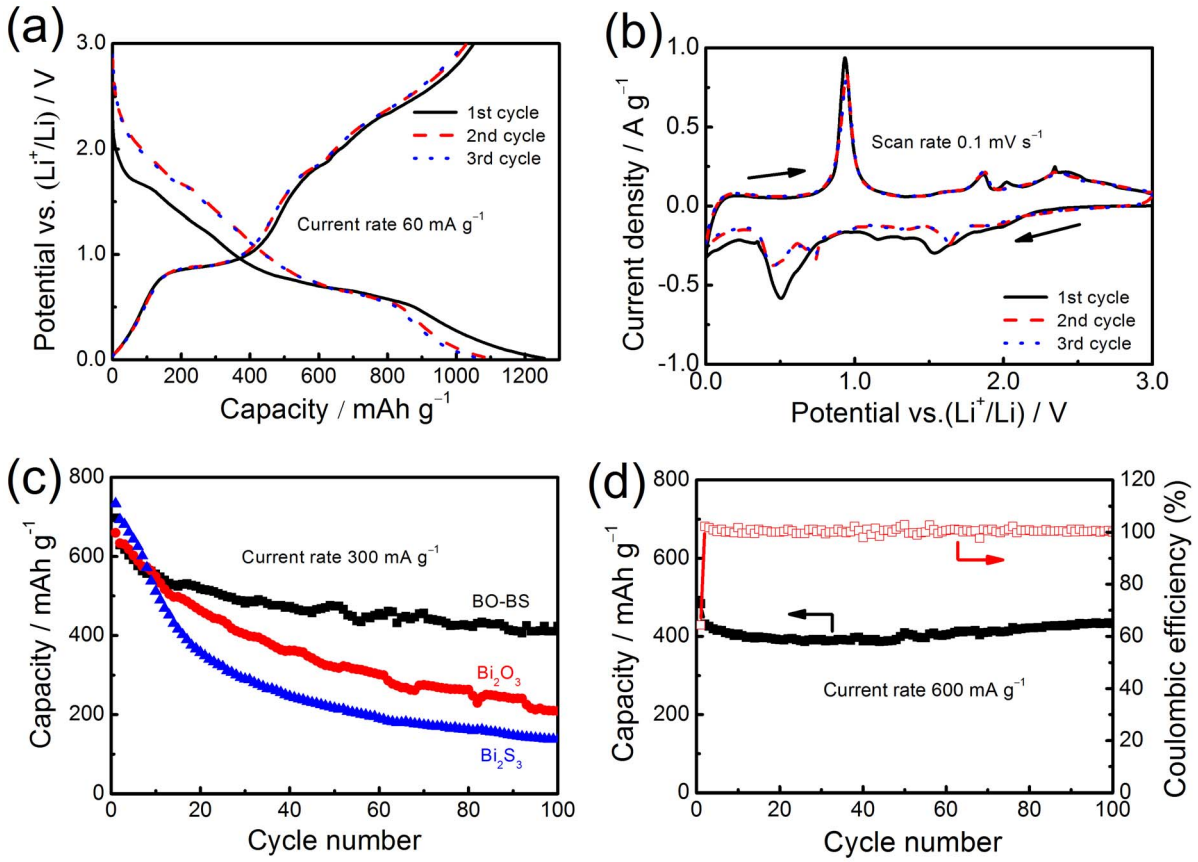

Figure 3 | (a) Charge and discharge profiles and (b) cyclic voltammogram curves of BO-BS heterostructure upon initial cycles. (c) Cycling comparison of BO-BS heterostructure, Bi_2S_3, and Bi_2O_3 at 300 mA g^{-1}. (d) Cycling performance of BO-BS heterostructure at 600 mA g^{-1}.

Figure 3b. Interestingly, Li uptake and release in the BO-BS show a stepwise reaction characteristic. In the cathodic process, two prominent peaks are located at 1.53 and 0.51 V, respectively. The peak at 1.53 V represents the reduction of Bi_2O_3 and Bi_2S_3 by Li (conversion process), while the other may be ascribed to Bi alloying Li to generate Li_3Bi. Reversely, the dealloying of Li_3Bi occurs at 0.93 V, while the recovery of Bi_2O_3 and Bi_2S_3 at 1.87 and 2.34 V in the anodic process[15]. In the following cycle, the CV curves slightly evolve, featuring the splitting of the alloying peak at 0.51 V and disappearance of anodic peak at 2.01 V. This evolution reflects possible structural transformation and irreversible lithium loss, which may be associated with deactivation of conversion product and side reactions as well[7].

Benefiting from the unique heterostructure design, the BO-BS exhibits impressive cycling stability, as shown in Figure 3c and d. The BO-BS retains 423 mAh g^{-1} after 100 continuous cycles at a rate of 300 mA g^{-1}, drastically outperforming Bi_2O_3 and Bi_2S_3 (fabricated according to previous work[5]) components (Figure 3c) and numerous bismuth based electrodes[6,30–32]. For instance, Bi_2S_3/C meshes only maintained 362 mAh g^{-1} over 40 cycles under the same test condition[6]. Figure 3d indicates that the heterostructure sustains a better cyclability at a higher rate, affording a capacity of 433 mAh g^{-1} (66% of the available 658 mAh g^{-1}) over 100 cycles at 600 mA g^{-1}. The improved stability at higher rate may be due to suppressed side reactions at low potential, which are time-dependent. At high rates, the electrodes experience short duration at low potential and thus the capacity fading can be reduced. To understand the durable cycling behaviour, the electrochemical impedance spectroscopy (EIS) of the heterostructure electrode at different cycling stage was conducted. The spectra indicate that negligible variation occurs after 100 cycling (Figure S4), suggesting that the electrochemical Li storage in the heterostructure is reversible and sustainable.

In addition, the unique BO-BS exhibits remarkably high rate capability, as presented in Figure 4a. At rates of 300, 600, 1200 and 3000 mA g^{-1}, the BO-BS affords capacities of 823, 710, 582, and 419 mAh g^{-1} (taking the 2nd cycle value at each rate), respectively. At a high rate of 6 A g^{-1}, it is still capable of delivering 295 mAh g^{-1}. Importantly, with the decrease of current rates, the capacity of the heterostructure increases accordingly, and a high value of 734 mAh g^{-1} is restored at 120 mA g^{-1}. The high rate behaviour can be further explored by the CV measurement. Figure 4b indicates that the heterostructure can sustain rapid potential sweep. Even at a fast sweep rate of 10.0 mV s^{-1}, the BO-BS still retains the basic CV profile, suggesting that the electrochemical Li storage has barely been restricted by the transport of electrons and Li ions. These results indicate that our engineered BO-BS outperforms most reported Bi_2O_3 and Bi_2S_3 materials[4–8,30–33], and is comparable to some well-designed sulfides such as Sb_2S_3@graphene[34] and SnS@CNT[35], suggesting the great potentiality of such heterostructures.

Discussion

Such an outstanding Li-storage property may arise from the unique heterogeneous architecture. Both Bi_2O_3 and Bi_2S_3 sheets show a thickness of about several nanometers, which greatly reduces the electron and ion transport length and charge transfer resistance. Also, corrugated sheets provide large accessible surface area for fast charge transfer and Li ion transport, which lowers the actual areal current flow and polarization. In addition, more conductive Bi_2S_3 sheets can serve as efficient electron transport pathway, which decreases the internal resistance of Bi_2O_3 electrodes and enables fast charge flow to meet high-rate charge and discharge. Furthermore, the unique heterogeneous architecture also effectively prevents the aggregation of nanosheets and consequently, retaining highly accessible area for Li uptake/release upon cycling.

To further elucidate the electrochemical process, the heterostructure electrode was held at different stage of the initial cycle: (i) discharge to 1 V, (ii) fully discharge to 0 V, and (iii) recharge to 3 V after full discharge. The cells were dismantled in a glove box, washed with dimethyl carbonate, and then subject to XRD and SEM tests. Figure S5 shows the XRD results for the electrode at different stages. The fresh electrode shows crystalline Bi_2O_3 and Bi_2S_3 phases, which disappear when the electrodes are discharged and/or recharged, suggesting that the material becomes amorphous after Li uptake and/or release. When the fully discharged electrode was exposed to air, diffraction peaks due to crystalline Li_2SO_4 emerge, which is due to the reaction between Li_2S and oxygen. This indicates that Li uptake really occurs for the electrochemical Li storage process. Figure S6 shows SEM images of the fresh and discharged BO-BS electrodes. The fresh electrode (Figure S6a) is smooth, while large elongated particles and voids are observed after the electrode was discharging to 0 V (Figure S6b). This is consistent with the fact that a large amount of Li is adsorbed from the reaction mechanism.

In conclusion, a unique heterostructure consisting of Bi_2O_3 and Bi_2S_3 nanosheets was readily fabricated via hydrolysis of $Bi(NO_3)_3 \cdot 5H_2O$ followed by sulfurization. The resulting BO-BS heterostructure features large surface area, enriched mesopores and intrinsic flexibility, which endow the material with superior Li storage capability. The heterostructures exhibit a high Coulombic efficiency (83.7%), stable capacity delivery (433 mAh g^{-1} over 100 cycles at 600 mA g^{-1}) and remarkable rate capability (295 mAh g^{-1} at 6 A g^{-1}), notably outperforming reported bismuth based materials. This work suggests that constructing heterostructure could be a promising strategy towards high-performance electrodes for rechargeable batteries.

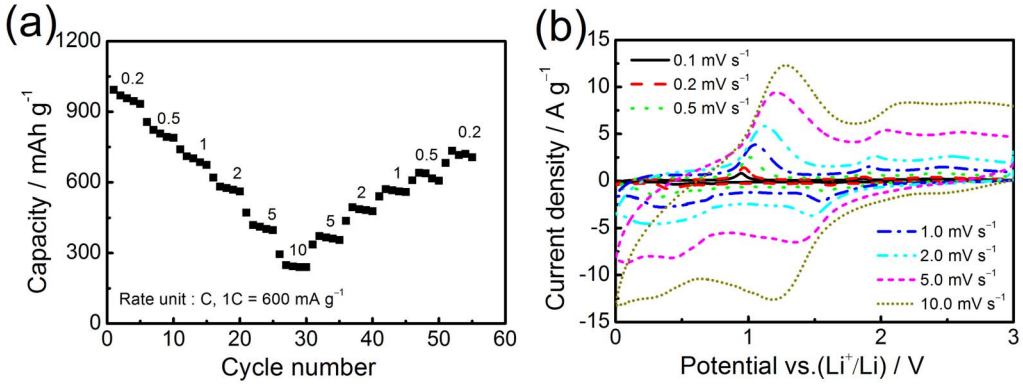

Figure 4 | (a) Cycling performance of BO-BS heterostructure at various current rates. (b) Cyclic voltammograms of BO-BS heterostructure at various sweep rates.

Methods

Sample preparation. The Bi_2O_3-Bi_2S_3 heterostructure was prepared using a facile sonochemical method[5]. In a typical operation, 0.35 mmol cetyltrimethyl ammonium bromide (CTAB, Sinopharm Chemicals) and 1.0 mmol thioacetamide (TAA, Sinopharm Chemicals) was dissolved in 40 ml water by sonication for 15 min. Then to this solution a 0.5 mmol $Bi(NO_3)_3{\cdot}5H_2O$ (in 5 ml of 0.4 M HNO_3) was added dropwise. After further agitation for 3 hours, the resulting precipitation was collected by centrifugation, washed repeatedly with water and ethanol, and dried at 60°C overnight. As a comparison, free Bi_2O_3 sample was also prepared via the similar process without using TAA.

Characterization. Structure of as-prepared products was identified by X-ray diffraction (XRD, Rigaku Dmax-2400 automatic diffractometer). Morphology was observed by scanning electron microscopy (SEM, Hitachi S-4800) equipped with energy dispersive X-ray spectroscopy (EDX, Oxford) and transmission electron microscopy (TEM, FEI Tecnai G2 T20). The materials were further characterized by Fourier transform infrared spectroscopy (FTIR, Bruker Tensor 27), thermogravimetry and differential thermal analysis (TG-DTA, Seko TG/DTA-7300), and nitrogen adsorption and desorption (Micromeritics Tristar 3020).

Electrochemical Li storage evaluation. Li storage performance of the heterostructure was electrochemically evaluated on coin-type 2032 cells. Prior to testing, the heterostructure material was heated at 200°C for 1 hour under Ar atmosphere. The working electrodes are composed of 70% active material, 20% Super-P-Li conductive carbon, and 10% polyvinylidene fluoride binder. The mass loading of active materials is about 1.5 mg cm^{-2}. The counter and reference electrode are Li metal foil, the electrolyte is 1 M $LiPF_6$ solution in ethylene carbonate and dimethyl carbonate (1 : 1 by volume), and the separator is glass microfiber (Whatman). Cells were assembled in an Ar-filled glove box (MBraun) with both water and oxygen concentration below 1 ppm. Cyclic voltammetry (CV) and electrochemical impedance spectroscopy (EIS) were measured on a Zennium electrochemical workstation (Zahner). Galvanostatic tests were performed on a LAND battery test system (Jinnuo) at room temperature.

1. Manthiram, A., Fu, Y. & Su, Y.-S. In Charge of the World: Electrochemical Energy Storage. *J. Phys. Chem. Lett.* **4**, 1295–1297 (2013).
2. Park, C.-M., Kim, J.-H., Kim, H. & Sohn, H.-J. Li-alloy based anode materials for Li secondary batteries. *Chem. Soc. Rev.* **39**, 3115 (2010).
3. Park, C.-M., Yoon, S., Lee, S.-I. & Sohn, H.-J. Enhanced electrochemical properties of nanostructured bismuth-based composites for rechargeable lithium batteries. *J. Power Sources* **186**, 206–210 (2009).
4. Jung, H., Park, C.-M. & Sohn, H.-J. Bismuth sulfide and its carbon nanocomposite for rechargeable lithium-ion batteries. *Electrochim. Acta* **56**, 2135–2139 (2011).
5. Ni, J. *et al.* Strongly coupled Bi_2S_3@CNT hybrids for robust lithium storage. *Adv. Energy Mater.* **4**, 1400798 (2014).
6. Zhao, Y. *et al.* One-pot facile fabrication of carbon-coated Bi_2S_3 nanomeshes with efficient Li-storage capability. *Nano Res.* **7**, 765–773 (2014).
7. Zhao, Y. *et al.* Branch-structured Bi_2S_3-CNT hybrids with improved lithium storage capability. *J. Mater. Chem. A* **2**, 13854–13858 (2014).
8. Li, Y. *et al.* Bismuth oxide: a new lithium-ion battery anode. *J. Mater. Chem. A* **1**, 12123–12127 (2013).
9. Drache, M., Roussel, P. & Wignacourt, J. P. Structures and oxide mobility in Bi-Ln-O materials: heritage of Bi_2O_3. *Chem. Rev.* **107**, 80–96 (2007).
10. Li, L., Yang, Y. W., Li, G. H. & Zhang, L. D. Conversion of a Bi nanowire array to an array of Bi-Bi_2O_3 core-shell nanowires and Bi_2O_3 nanotubes. *Small* **2**, 548–553 (2006).
11. Zhou, L., Wang, W., Xu, H., Sun, S. & Shang, M. Bi_2O_3 hierarchical nanostructures: controllable synthesis, growth mechanism, and their application in photocatalysis. *Chem. Eur. J.* **15**, 1776–1782 (2009).
12. Moniz, S. J. A., Blackman, C. S., Carmalt, C. J. & Hyett, G. MOCVD of crystalline Bi_2O_3 thin films using a single-source bismuth alkoxide precursor and their use in photodegradation of water. *J. Mater. Chem.* **20**, 7881–7886 (2010).
13. Liu, F.-A., Yang, Y.-C., Liu, J., Huang, W. & Li, Z.-L. Preparation of Bi_2O_3@Bi_2S_3 core–shell nanoparticle assembled thin films and their photoelectrochemical and photoresponsive properties. *J. Electroanal. Chem.* **665**, 58–62 (2012).
14. Fiordiponti, P., Pistoia, G. & Temperoni, C. Behavior of Bi_2O_3 as a cathode for lithium cells. *J. Electrochem. Soc.* **125**, 14–17 (1978).
15. Yuan, S. *et al.* Engraving copper foil to give large-scale binder-free porous CuO arrays for a high-performance sodium-ion battery anode. *Adv. Mater.* **26**, 2273–2279, 2284 (2014).
16. Jiang, X. *et al.* Rational growth of branched nanowire heterostructures with synthetically encoded properties and function. *Proc. Natl. Acad. Sci.* **108**, 12212–12216 (2011).
17. Chu, H. B., Wei, L., Cui, R. L., Wang, J. Y. & Li, Y. Carbon nanotubes combined with inorganic nanomaterials: Preparations and applications. *Coord. Chem. Rev.* **254**, 1117–1134 (2010).
18. Xia, H., Ragavendran, K. R., Xie, J. & Lu, L. Ultrafine $LiMn_2O_4$/carbon nanotube nanocomposite with excellent rate capability and cycling stability for lithium-ion batteries. *J. Power Sources* **212**, 28–34 (2012).
19. Wang, Y. G., Hong, Z. S., Wei, M. D., Xia, Y. Y. Layered $H_2Ti_6O_{13}$-Nanowires: A new promising pseudocapacitive material in non-aqueous electrolyte. *Adv. Funct. Mater.* **22**, 5185–5193 (2012).
20. Ni, J. F., Han, Y. H., Gao, L. J. & Lu, L. One-pot synthesis of CNT-wired $LiCo_{0.5}Mn_{0.5}PO_4$ nanocomposites. *Electrochem. Commun.* **31**, 84–87 (2013).
21. Guan, C. *et al.* Highly stable and reversible lithium storage in SnO_2 nanowires surface coated with a uniform hollow shell by atomic layer deposition. *Nano Lett* **14**, 4852–4858 (2014).
22. Wang, H., Chen, L., Feng, Y. & Chen, H. Exploiting core-shell synergy for nanosynthesis and mechanistic investigation. *Accounts Chem. Res.* **46**, 1636–1646 (2013).
23. Ni, J. *et al.* Carbon nanotube-wired and oxygen-deficient MoO_3 nanobelts with enhanced lithium-storage capability. *J. Power Sources* **247**, 90–94 (2014).
24. Luo, J. *et al.* Rationally designed hierarchical TiO_2@Fe_2O_3 hollow nanostructures for improved lithium ion storage. *Adv. Energy Mater.* **3**, 737–743 (2013).
25. Chen, Z. *et al.* Core–shell MoO_3–MoS_2 nanowires for hydrogen evolution: A functional design for electrocatalytic materials. *Nano Lett.* **11**, 4168–4175 (2011).
26. Yin, Z. *et al.* Preparation of MoS_2-MoO_3 hybrid nanomaterials for light-emitting diodes. *Angew. Chem. Int. Ed.* **53**, 1–7 (2014).
27. Xia, X. *et al.* Synthesis of free-standing metal sulfide nanoarrays via anion exchange reaction and their electrochemical energy storage application. *Small* **10**, 766–773 (2014).
28. Lu, F. *et al.* Synthesis of Bi_2S_3–Bi_2O_3 composites and their enhanced photosensitive properties. *RSC Adv.* **4**, 5666–5670 (2014).
29. Ni, J. F., Huang, Y. Y. & Gao, L. J. A high-performance hard carbon for Li-ion batteries and supercapacitors application. *J. Power Sources* **223**, 306–311 (2013).
30. Ma, J. *et al.* Ionic liquids-assisted synthesis and electrochemical properties of Bi_2S_3 nanostructures. *Cryst Eng Comm* **13**, 3072–3079 (2011).
31. Jin, R., Li, G., Liu, J. & Yang, L. A facile route to flowerlike Bi_2S_3 constructed by polycrystalline nanoplates with enhanced electrochemical properties. *Eur. J. Inorg. Chem.* **2013**, 5400–5407 (2013).
32. Zhang, Z. *et al.* Synthesis of bismuth sulfide/reduced graphene oxide composites and their electrochemical properties for lithium ion batteries. *Electrochim. Acta* **114**, 88–94 (2013).
33. Jin, R. C., Xu, Y. B., Li, G. H., Liu, J. S. & Chen, G. Hierarchical chlorophytum-like Bi_2S_3 architectures with high electrochemical performance. *Int. J. Hydrogen Energy* **38**, 9137–9144 (2013).
34. Prikhodchenko, P. V. *et al.* Conversion of hydroperoxoantimonate coated graphenes to Sb_2S_3@Graphene for a superior lithium battery anode. *Chem. Mater.* **24**, 4750–4757 (2012).
35. Zhai, C., Du, N., Zhang, H., Yu, J. & Yang, D. Multiwalled carbon nanotubes anchored with SnS_2 nanosheets as high-performance anode materials of lithium-ion batteries. *ACS Appl. Mater. Interfaces* **3**, 4067–4074 (2011).

Acknowledgments

Support of this work by the National Natural Science Foundation of China (51302181) and China Postdoctoral Science Foundation (2014M551647) is acknowledged.

Author contributions

J.N. conceived and designed the experiments. T.L. and Y.Z. carried out the material synthesis and conducted the characterization. L.G. and J.N. wrote the manuscript. All the authors participated in discussions of the research.

Additional information

Supplementary information accompanies this paper at http://www.nature.com/scientificreports

Competing financial interests: The authors declare no competing financial interests.

How to cite this article: Liu, T., Zhao, Y., Gao, L. & Ni, J. Engineering Bi_2O_3-Bi_2S_3 heterostructure for superior lithium storage. *Sci. Rep.* 5, 9307; DOI:10.1038/srep09307 (2015).